Cardiovascular Research (2017) **113**, 102–111
doi:10.1093/cvr/cvw234

Multilevel analyses of *SCN5A* mutations in arrhythmogenic right ventricular dysplasia/ cardiomyopathy suggest non-canonical mechanisms for disease pathogenesis

Anneline S.J.M. te Riele[1,2,3†], Esperanza Agullo-Pascual[4†], Cynthia A. James[1], Alejandra Leo-Macias[4], Marina Cerrone[4], Mingliang Zhang[4], Xianming Lin[4], Bin Lin[4], Eli Rothenberg[5], Nara L. Sobreira[6], Nuria Amat-Alarcon[1], Roos F. Marsman[7], Brittney Murray[1], Crystal Tichnell[1], Jeroen F. van der Heijden[2], Dennis Dooijes[8], Toon A.B. van Veen[9], Harikrishna Tandri[1], Steven J. Fowler[4], Richard N.W. Hauer[2,3], Gordon Tomaselli[1], Maarten P. van den Berg[10], Matthew R.G. Taylor[11], Francesca Brun[12], Gianfranco Sinagra[12], Arthur A.M. Wilde[7], Luisa Mestroni[11], Connie R. Bezzina[7], Hugh Calkins[1], J. Peter van Tintelen[10,13,14], Lei Bu[1,4]*, Mario Delmar[1,4]*, and Daniel P. Judge[1]*

[1]Department of Medicine, Division of Cardiology, Johns Hopkins University School of Medicine, 1800 Orleans Street, Baltimore, MD, USA; [2]Division of Cardiology, University Medical Center Utrecht, Heidelberglaan 100, Utrecht, the Netherlands; [3]Netherlands Heart Institute, Moreelsepark 1, Utrecht, the Netherlands; [4]Leon H. Charney Division of Cardiology, New York University School of Medicine, 550 First Avenue, New York, NY, USA; [5]Department of Biochemistry and Molecular Pharmacology, NYU-SoM, 522 First Avenue, MSB 3rd Floor, New York, New York 10016, USA; [6]McKusick-Nathans Institute of Genetic Medicine, Johns Hopkins University School of Medicine, 720 Rutland Avenue, Baltimore, MD, USA; [7]Heart Centre, Department of Clinical and Experimental Cardiology, Academic Medical Center, Meibergdreef 9, Amsterdam, the Netherlands; [8]Department of Medical Genetics, University Medical Center Utrecht, Heidelberglaan 100, Utrecht, the Netherlands; [9]Department of Medical Physiology, Division of Heart and Lungs, University Medical Center Utrecht, Yalelaan 50, Utrecht, the Netherlands; [10]Department of Cardiology, University Medical Center Groningen, University of Groningen, Hanzeplein 1, Groningen, the Netherlands; [11]Cardiovascular Institute and Adult Medical Genetics, University of Colorado Denver, 12605 E 16th Avenue, Aurora, CO, USA; [12]Cardiovascular Department, Ospedali Riuniti and University of Trieste, Via Farneto 3, Trieste, Italy; [13]Department of Clinical Genetics, Academic Medical Center Amsterdam, University of Amsterdam, Meibergdreef 9, Amsterdam, the Netherlands; and [14]Department of Genetics, University of Groningen, University Medical Center Groningen, Hanzeplein 1, Groningen, the Netherlands

Received 20 June 2016; revised 21 August 2016; editorial decision 1 November 2016; accepted 14 November 2016

Time of primary review: 4 days

Aims Arrhythmogenic Right Ventricular Dysplasia/Cardiomyopathy (ARVD/C) is often associated with desmosomal mutations. Recent studies suggest an interaction between the desmosome and sodium channel protein $Na_v1.5$. We aimed to determine the prevalence and biophysical properties of mutations in *SCN5A* (the gene encoding $Na_v1.5$) in ARVD/C.

Methods and results We performed whole-exome sequencing in six ARVD/C patients (33% male, 38.2 ± 12.1 years) without a desmosomal mutation. We found a rare missense variant (p.Arg1898His; R1898H) in *SCN5A* in one patient. We generated induced pluripotent stem cell-derived cardiomyocytes (hIPSC-CMs) from the patient's peripheral blood mononuclear cells. The variant was then corrected (R1898R) using Clustered Regularly Interspaced Short Palindromic Repeats/Cas9 technology, allowing us to study the impact of the R1898H substitution in the same cellular background. Whole-cell patch clamping revealed a 36% reduction in peak sodium current ($P = 0.002$); super-resolution fluorescence microscopy showed reduced abundance of $Na_V1.5$ ($P = 0.005$) and N-Cadherin ($P = 0.026$) clusters at the intercalated disc. Subsequently, we sequenced *SCN5A* in an additional 281 ARVD/C patients (60% male, 34.8 ± 13.7 years, 52% desmosomal mutation-carriers). Five (1.8%) subjects harboured a putatively pathogenic *SCN5A* variant (p.Tyr416Cys, p.Leu729del, p.Arg1623Ter, p.Ser1787Asn, and p.Val2016Met). *SCN5A* variants were

*Corresponding authors. Tel: +1 410 614 3085; fax: +1 410 367 2149, E-mail: djudge@jhmi.edu; Tel: +1 212 263 9492; fax: +1 212 263 4129, E-mail: mario.delmar@nyumc.org; Tel: +1 212 263 9139; fax: +1 212 263 9139, E-mail: lei.bu@med.nyu.edu

† These authors contributed equally to the manuscript.

associated with prolonged QRS duration (119 ± 15 vs. 94 ± 14 ms, $P < 0.01$) and all *SCN5A* variant carriers had major structural abnormalities on cardiac imaging.

Conclusions Almost 2% of ARVD/C patients harbour rare *SCN5A* variants. For one of these variants, we demonstrated reduced sodium current, $Na_v1.5$ and N-Cadherin clusters at junctional sites. This suggests that $Na_v1.5$ is in a functional complex with adhesion molecules, and reveals potential non-canonical mechanisms by which $Na_v1.5$ dysfunction causes cardiomyopathy.

Keywords Arrhythmogenic right ventricular cardiomyopathy • SCN5A • Genetics • Cardiomyopathy • Ion channel electrophysiology

1. Introduction

The cardiac intercalated disc hosts a molecular network that integrates intercellular adhesion, electrical coupling, and excitability at the site of contact between cardiomyocytes. Disruption of this complex undermines the integrity of the myocardium, as demonstrated by various disease states associated with intercalated disc remodelling. One of these diseases is Arrhythmogenic Right Ventricular Dysplasia/Cardiomyopathy (ARVD/C), an inherited disorder characterized by ventricular arrhythmias and fibrofatty replacement of predominantly the right ventricular (RV) myocardium. Mutations in genes encoding the cardiac desmosome are identified in the majority of affected patients,[1] although the genetic basis extends beyond desmosomal proteins.[2–4] Of particular interest in this regard is $Na_v1.5$, the pore-forming subunit of the voltage-gated cardiac sodium channel. Early studies showed that the desmosomal protein plakophilin-2 (*PKP2*) co-precipitates with $Na_v1.5$, and that loss of *PKP2* expression alters the amplitude and kinetics of the sodium current (I_{Na}).[3,5] Furthermore, mutations in *PKP2* have been associated with a sodium channelopathy phenotype,[6] while decreased immunoreactive $Na_v1.5$ protein has been detected in the majority of human ARVD/C heart samples.[7] These observations indicate a close functional association between $Na_v1.5$ and mechanical junction proteins. The concept is further validated by observations that $Na_v1.5$ co-precipitates with the adherens junction protein N-Cadherin,[5] and by super-resolution microscopy studies demonstrating the presence of 'adhesion/excitability' nodes formed by aggregates of $Na_v1.5$ and N-Cadherin.[8] Likewise, we postulated that mutations in the voltage-gated sodium channel complex may be part of the molecular substrate underlying ARVD/C.

2. Methods

2.1 Study population and molecular genetic screening

We first screened the entire exome for mutations among a 'discovery cohort' of six unrelated Caucasian patients with a clinical diagnosis of ARVD/C according to the 2010 Task Force Criteria[9] and without mutations in the ARVD/C-associated desmosomal genes (*PKP2, DSC2, DSG2, DSP*, and *JUP*). All individuals underwent whole-exome sequencing using the Illumina HiSeq2000 platform. We used the human reference genome GRCh37/hg19 for mapping.[10] Detailed genetic screening methodology for the discovery cohort is described in the Supplementary material online.

We subsequently analysed *SCN5A* in a multicentre transatlantic 'validation cohort' of 281 unrelated patients who had a clinical diagnosis of ARVD/C according to the 2010 Task Force Criteria[9] and who underwent sequencing for the ARVD/C-associated desmosomal genes (*PKP2, DSC2, DSG2, DSP*, and *JUP*). Patients were divided into those with a pathogenic desmosomal mutation ($n = 146$) and those without a pathogenic desmosomal mutation ($n = 135$). Pathogenicity of desmosomal mutations was determined as done previously.[11] Most participants were Caucasian ($n = 276$); four were Asian and one was African American. Detailed genetic screening methodology for the validation cohort is described in the Supplementary material online.

Potentially causal variants were identified using standard filtering criteria. Variants were excluded if they had a minor allele frequency (MAF) >1% in the Exome Aggregation Consortium, Cambridge, MA, Exome Variant Server (release ESP6500SI-V2), or 1000 Genomes Project, and/or if they were present in dbSNP 137. We also excluded all variants with an SIFT score >0.03 and/or a Polyphen2 score of <0.90. Nucleic acid deviations were compared with the reference sequence for *SCN5A* (NM_198056.2). All mutations were confirmed by Sanger sequencing. The study complies with the Declaration of Helsinki and a locally appointed ethics committee approved the research protocol. Informed consent was obtained from all participants.

2.2 Generation of induced pluripotent stem cell-derived cardiomyocytes

We assessed the cellular and molecular phenotype of the *SCN5A* mutation identified in our discovery cohort [p.Arg1898His (c.5693G > A)] in induced pluripotent stem cell-derived cardiomyocytes (IPSC-CMs) that were derived from the patient's peripheral blood mononuclear cells. Detailed methodology is described in the Supplementary material online. T-cells-enriched peripheral blood mononuclear cells from the patient and two normal controls were used for human IPSC derivation using standard techniques (CytoTune-iPS 2.0 Sendai Reprogramming Kit, Invitrogen, Carlsbad CA, USA). Human IPSC clones were picked, cultured, and expanded on the mouse embryonic fibroblasts while following the manufacturer's instructions.

2.3 Whole-cell patch clamping and three-dimensional super-resolution fluorescence microscopy

Whole-cell I_{Na} recordings were conducted using standard protocols that are described in the Supplementary material online. In addition, we performed two-colour ($Na_v1.5$ and N-Cadherin) three-dimensional imaging by direct stochastic optical reconstruction microscopy. Our spatial resolution in the X–Y plane was ~20 nm. Detailed methods are described in Leo-Macias *et al.*[8]; a brief description is provided in the Supplementary material online.

Table 1 Summary of *SCN5A* rare variants associated with ARVD/C

Amino acid change	cDNA change	Exon	Type	Location	MAF (%) ExAC[a]	MAF (%) EVS[a]	Polyphen2 score	Polyphen2 prediction	SIFT score	SIFT prediction	Conservation (GERP)	References
Discovery cohort												
p.Arg1898His	c.5693G>A	28	Missense	C-terminus	0.007	0.0158	0.960	Probably damaging	0.03	Damaging	4.86	–
Validation cohort												
p.Tyr416Cys	c.1247A>G	10	Missense	IL I–II	0.008	0.008	1.0	Probably damaging	0	Damaging	5.54	31
p.Leu729del	c.2184–2186 del	14	In-frame deletion	DII S1	–	–	–	–	–	–	–	–
p.Arg1623Ter	c.4867C>T	28	Stop codon	DIV S4 voltage sensor	–	–	–	–	–	–	–	–
p.Ser1787Asn	c.5360G>A	28	Missense	C-terminus	0.0604	0.0692	0.976	Probably damaging	0	Damaging	4.82	22, 25–27[b]
p.Val2016Met	c.6048G>A	28	Missense	C-terminus	0.0037	–	0.999	Probably damaging	0	Damaging	3.59	28, 29

ARVD/C, arrhythmogenic right ventricular dysplasia/cardiomyopathy; DII, Domain II; EVS, exome variant server; ExAc, Exome Aggregation Consortium; GERP, Genomic Evolutionary Rate Profiling; IL, interdomain linker; MAF, minor allele frequency; S1, transmembrane spanning segment 1.
[a]Accessed 30 July 2016.
[b]Although previous studies have identified this variant in controls,[22,25] it has also been observed in affected individuals,[27] and a recent study described an abnormal biophysical phenotype that depends on splice variant and pH.[26]

2.4 Genetic correction of the *SCN5A* mutation in human IPSC-CMs

The p.Arg1898His mutation in patient-specific IPSC-CMs was corrected using Clustered Regularly Interspaced Short Palindromic Repeats (CRISPR) with CRISPR-associated (Cas9) system, following a recently published protocol.[12] Successful correction of the p.Arg1898His mutation was confirmed by direct sequencing (see Supplementary material online, *Figure S1*), and off-target effects generated by CRISPR-Cas9 were evaluated to confirm that the rescued phenotype is a direct result of the genetic correction (see Supplementary material online, *Table S1*). Successfully corrected cell clones were selected for cardiac differentiation. Detailed methodology is described in the Supplementary material online.

2.5 Generation of HEK293 cells

HEK293 cells, derived from human embryonic kidney cells, were used to complement IPSC-CMs experiments. DNA plasmids containing cDNA for human *SCN5A* or mutant *SCN5A*-c.5693A were transfected into HEK293 cells using Lipofectamine 2000 reagent (Life Technologies, Carlsbad, CA, USA). Patch clamping was performed 48 h after transfection. Expression of the transfectant was confirmed by western blots for $Na_v1.5$ using a polyclonal $Na_v1.5$ antibody (Sigma, St. Louis, MO, USA). Please see the Supplementary material online for more details.

2.6 Statistical analysis

Continuous data were presented as mean ± standard deviation or median (inter-quartile range) and categorical variables as numbers (percentages). Continuous variables were compared using the independent Student's *t*-test or Mann–Whitney *U* test for comparison between two groups and analysis of variance or Kruskall–Wallis test for comparison between three groups. *Post hoc* tests were performed by Bonferroni correction to account for multiple comparisons. Categorical data were compared using χ^2 test or Fisher's exact test. Analyses were performed using STATA 13.1 (Stata Corp, College Station, TX, USA). A *P*-value <0.05 was considered statistically significant.

3. Results

3.1 Discovery cohort

3.1.1 Molecular genetic screening

We performed whole-exome sequencing in six unrelated ARVD/C patients [2 (33%) male, age at presentation 38.2 ± 12.1 years] who did not harbour a desmosomal mutation. A heterozygous *SCN5A* missense variant (c.5693G > A) was identified in a female patient, indicating the substitution of a highly conserved arginine to histidine at position 1898 (p.Arg1898His). Detailed information of the variant is shown in *Table 1*. The variant was rare, with an MAF of 0.007% (present in 8/12,0768 alleles reported in the Exome Aggregation Consortium, http://exac.broadinstitute.org, accessed 30 July 2016). It localized to a highly conserved region of the C-terminus of $Na_v1.5$ (Genomic Evolutionary Rate Profiling score 4.86). The variant was predicted pathogenic by SIFT (score 0.03) and Polyphen2 (score 0.960). Supplementary material online, *Table S2* includes other variants identified on whole-exome sequencing in this individual, with the factors that led to prioritizing them below *SCN5A*.

3.1.2 Clinical evaluation

The patient presented at age 29 years with ventricular tachycardia (VT) of left bundle branch block (LBBB) inferior axis morphology after playing soccer. *Figure 1* shows a summary of her clinical evaluation. ARVD/C diagnosis was made based on T-wave inversions in V1-2 (minor TFC), RV dyskinesia with RV end-diastolic volume 128 mL/m^2 (major TFC), and LBBB VT (minor TFC). The PR (145 ms), QRS (90 ms), and QTc (375 ms) intervals were within normal limits. The patient did not have a history of spontaneous ST-segment elevation in the right precordial

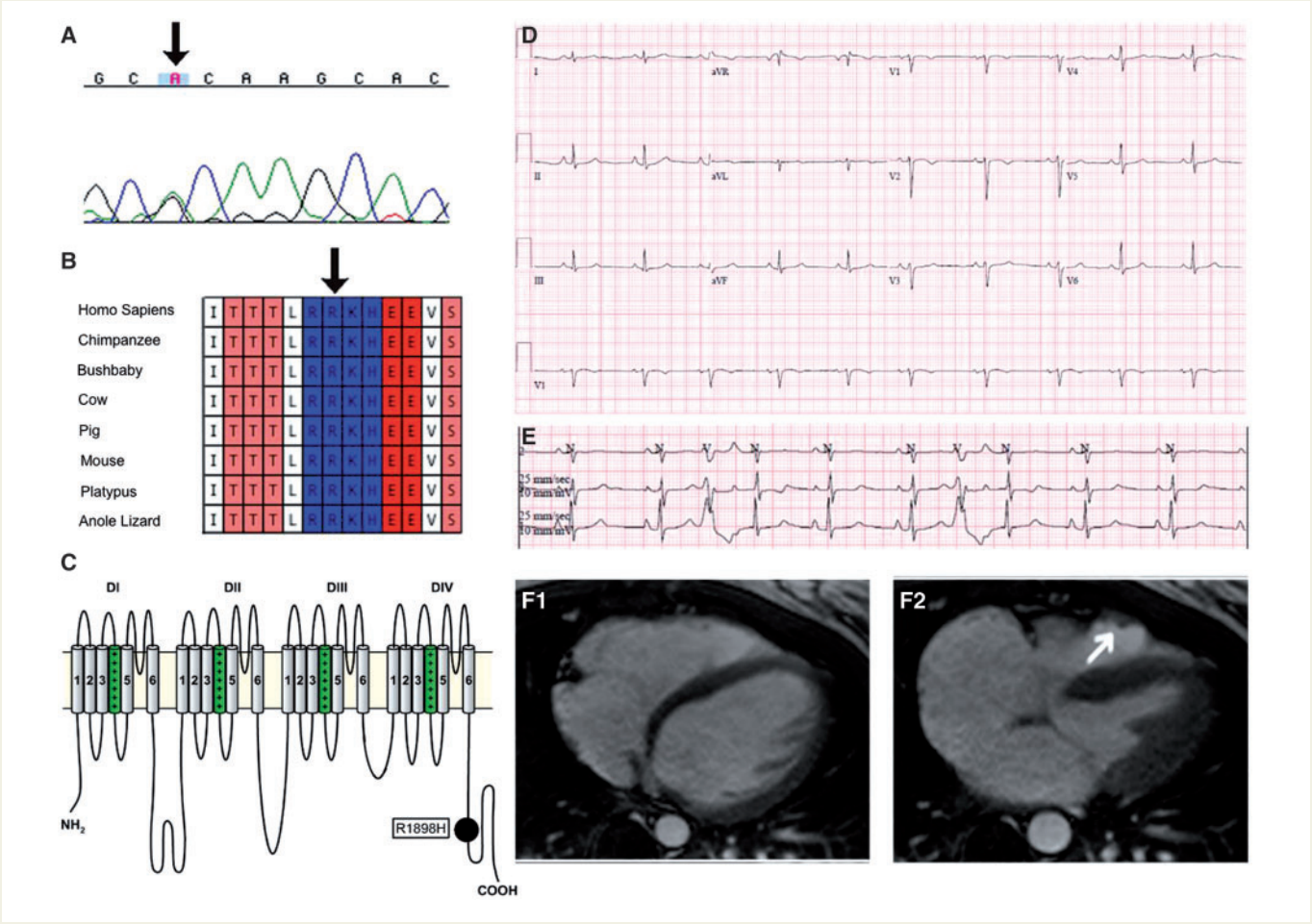

Figure 1 Genetic and clinical evaluation of the 29-year-old female ARVD/C patient harbouring an *SCN5A* mutation (p.Arg1898His) identified through whole-exome sequencing. (*A*) Whole-exome sequencing revealed a heterozygous G>A missense mutation at position 5693. This variant located to a highly conserved region of the sodium channel (*B*) in the C-terminal domain (CTD) (*C*). 12-lead electrocardiography showed T-wave inversions in V1–2 with normal conduction intervals (PR 145 ms; QRS 90 ms; QTc 375 ms) (*D*) and Holter monitoring revealed 217 PVCs/24 h (*E*). End-diastolic (*F1*) and end-systolic (*F2*) cardiac magnetic resonance images showed an enlarged right ventricle (end-diastolic volume 128 mL/m^2) and dyskinesia in the RV outflow tract (arrow, *F2*). Please also note biatrial enlargement (right atrium > left atrium), which is a common finding in ARVD/C cases.[30] Topology of $Na_v1.5$ obtained with kind permission of Oxford University Press (original manuscript Cardiovasc Res 2007;76:381–9).

leads; a pharmacological sodium blocker challenge was not performed. Family members were not amenable to genetic testing.

3.1.3 Functional characterization: biophysical effect on sodium channel

The consequence of the p.Arg1898His mutation on the biophysical and structural properties of $Na_v1.5$ was studied in IPSC-CM from the patient's peripheral blood mononuclear cells. Gene editing (CRISPR-Cas9) was used to generate a parallel hIPSC-CM line from the same patient, one in which the histidine in position 1898 was reversed back to arginine (p.Arg1898His reversed to p.Arg1898Arg). Using whole-cell patch clamp, we demonstrated that the peak I_{Na} density of cells carrying p.Arg1898His was 36% reduced when compared with those expressing the wild-type amino acid (p.Arg1898Arg) in the same position ($P = 0.002$; see *Figure 2A*). To document that the change in current amplitude is robust and independent of cell-type, we examined the properties of the sodium current generated by p.Arg1898Arg or p.Arg1898His in an exogenous cell system. For this purpose, we transiently transfected HEK293 cells with cDNA coding for *SCN5A*. Similar to the IPSC-CMs, the current density generated by a construct containing the *SCN5A* p.Arg1898His mutation was significantly reduced compared with wild-type *SCN5A* (p.Arg1898Arg) ($P = 0.002$; see *Figure 2B*). Both in the case of the hIPSC-CMs and in the HEK cells, the steady-state voltage dependence of inactivation was not affected by the mutation (*Figure 2C* and *D*).

3.1.4 Effect of mutation on intercalated disc organization

We examined the effects of the p.Arg1898His *SCN5A* mutation on intercalated disc organization by three-dimensional super-resolution fluorescence microscopy (3D-SRFM) (*Figure 3*). Cells used for 3D-SRFM were obtained and processed in parallel to those used for the patch clamp experiments. We focused our analysis on cells that showed a striated pattern of α-actinin staining. Data acquisition was limited to areas of cell–cell contact positive for N-Cadherin staining (*Figure 3A*). The same two cell populations characterized in terms of I_{Na} density (*Figure 2*) were studied. As shown in *Figure 3B*, the density of protein clusters of both

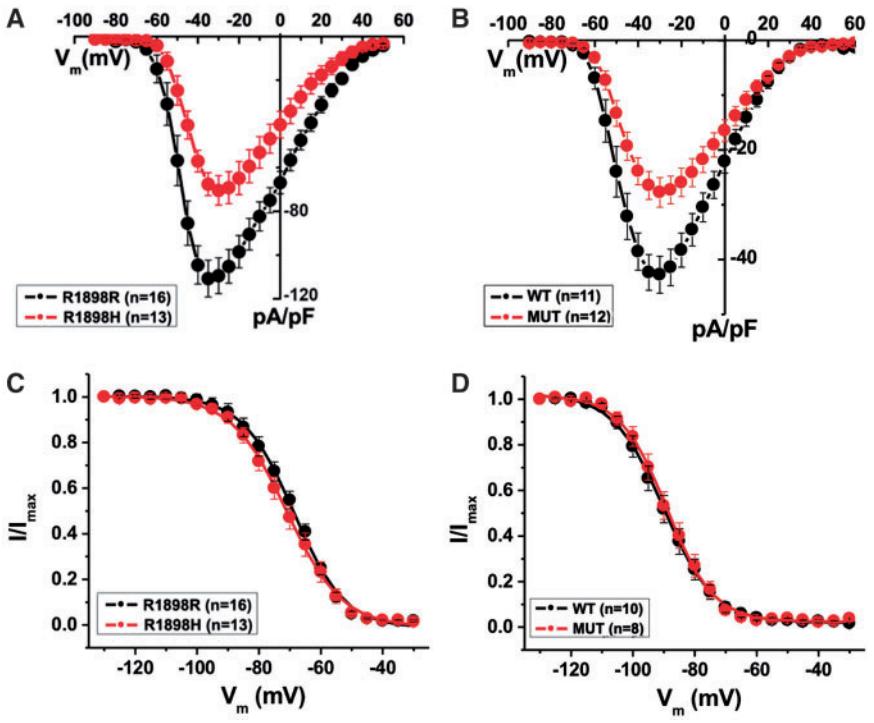

Figure 2 Biophysical effect of the *SCN5A* mutation on sodium current properties. (*A*) *I–V* relationship of I_{Na} in hIPSC-CMs from the ARVD/C patient (red) and cells from the same patient after gene-editing (black). $I_{Na,peak}$ -70.3 ± 6.7 (p.Arg1898His) vs. -109.4 ± 8.2 pA/pF (p.Arg1898Arg), equivalent to a 36% [100 - (-70.3/-109.4*100)] reduction in peak sodium current, $P = 0.002$ (Student's *t*-test). (*B*) *I–V* relationship of I_{Na} in HEK cells transiently transfected with the *SCN5A* mutant (red) and wild-type (black). $I_{Na,peak}$ -27.7 ± 2.7 (mutant) vs. -42.7 ± 3.4 pA/pF (wild-type), $P = 0.002$ (Student's *t*-test). (*C*) Voltage dependence of steady-state inactivation in IPSC-CMs from the ARVD/C patient (red) and cells from the same patient after gene-editing (black). $V_{1/2,inactivation}$ -70.9 ± 1.9 mV (p.Arg1898His) vs. -68.7 ± 0.9 mV (p.Arg1898Arg), $P > 0.05$ (Student's *t*-test). (*D*) Voltage dependence of steady-state inactivation in HEK cells transiently transfected with the *SCN5A* mutant (red) and wild-type (black). $V_{1/2,inactivation}$ -89.0 ± 1.3 mV (mutant) vs. -90.0 ± 1.2 mV (wild-type), $P > 0.05$ (Student's *t*-test).

$Na_V1.5$ ($P = 0.0054$) and N-Cadherin ($P = 0.026$) was larger in gene-edited cells, whereas cluster size was not dependent on whether arginine or histidine occupied position 1898 of $Na_v1.5$ ($P = 0.126$ for $Na_v1.5$ and $P = 0.536$ for N-Cadherin; *Figure 3C and D*). Overall, these results suggest that the p.Arg1898His *SCN5A* mutation associates with reduced average peak sodium current density and reduced density of $Na_v1.5$ and N-Cadherin clusters at the site of cell contact.

3.2 Validation cohort

To validate the presence of *SCN5A* variants in ARVD/C patients, we performed sequencing of *SCN5A* in a multicentre validation cohort of 281 unrelated ARVD/C patients [169 (60%) male, age at presentation 34.8 ± 13.7 years]. Approximately half ($n = 135$, 48%) of subjects did not harbour a mutation in any of the ARVD/C-associated desmosomal genes; the remainder ($n = 146$, 52%) carried a pathogenic desmosomal mutation (77% *PKP2*, see Supplementary material online, *Table S3*).

We identified a putatively pathogenic heterozygous *SCN5A* variant in 5/281 (1.8%) patients. Prevalence of *SCN5A* variants was 2.2% ($n = 3$/135) in those without a desmosomal mutation compared with 1.4% ($n = 2$/146) in those with a desmosomal mutation. A summary of *SCN5A* variants is shown in *Table 1*. All variants were rare (MAF ≤ 0.0692%; 4/5 variants with an MAF <0.05%) or novel, occurred in highly conserved region of the sodium channel, and were predicted pathogenic by SIFT and Polyphen2.

Table 2 shows detailed clinical data of the five *SCN5A* mutation carriers. All patients fulfilled ARVD/C diagnosis according to the 2010 diagnostic Task Force Criteria;[9] of note, they all had major structural abnormalities on cardiac imaging. One *SCN5A* mutation carrier (p.Tyr416Cys) also harboured a variant of uncertain significance in the *LMNA* gene [p.Arg190Gln (c.569G > A)] (see *Table 2* for details). Among *SCN5A* variant carriers, mean QRS duration was prolonged (119 ± 15 ms), whereas PR and QTc intervals were within normal limits (168 ± 19 and 416 ± 34 ms, respectively). None of the subjects had spontaneous ST-segment elevation. One *SCN5A* mutation carrier (p.Leu729del) underwent pharmacological sodium channel blocker challenge, which failed to unmask the electrocardiographic pattern of Brugada syndrome at peak intravenous ajmaline dose 1 mg/kg. As shown in *Figure 4*, an ARVD/C family history was observed in one *SCN5A* mutation carrier, in whom the variant (p.Leu729del) co-segregated with the phenotype with reduced penetrance. The other variant carriers did not have a family history of ARVD/C, although cardiac screening was limited.

3.3 Comparison of demographics and clinical phenotype by genotype

We compared the demographic and phenotypic characteristics of ARVD/C patients with an *SCN5A* variant with those with and without a desmosomal mutation. As shown in the Supplementary material online,

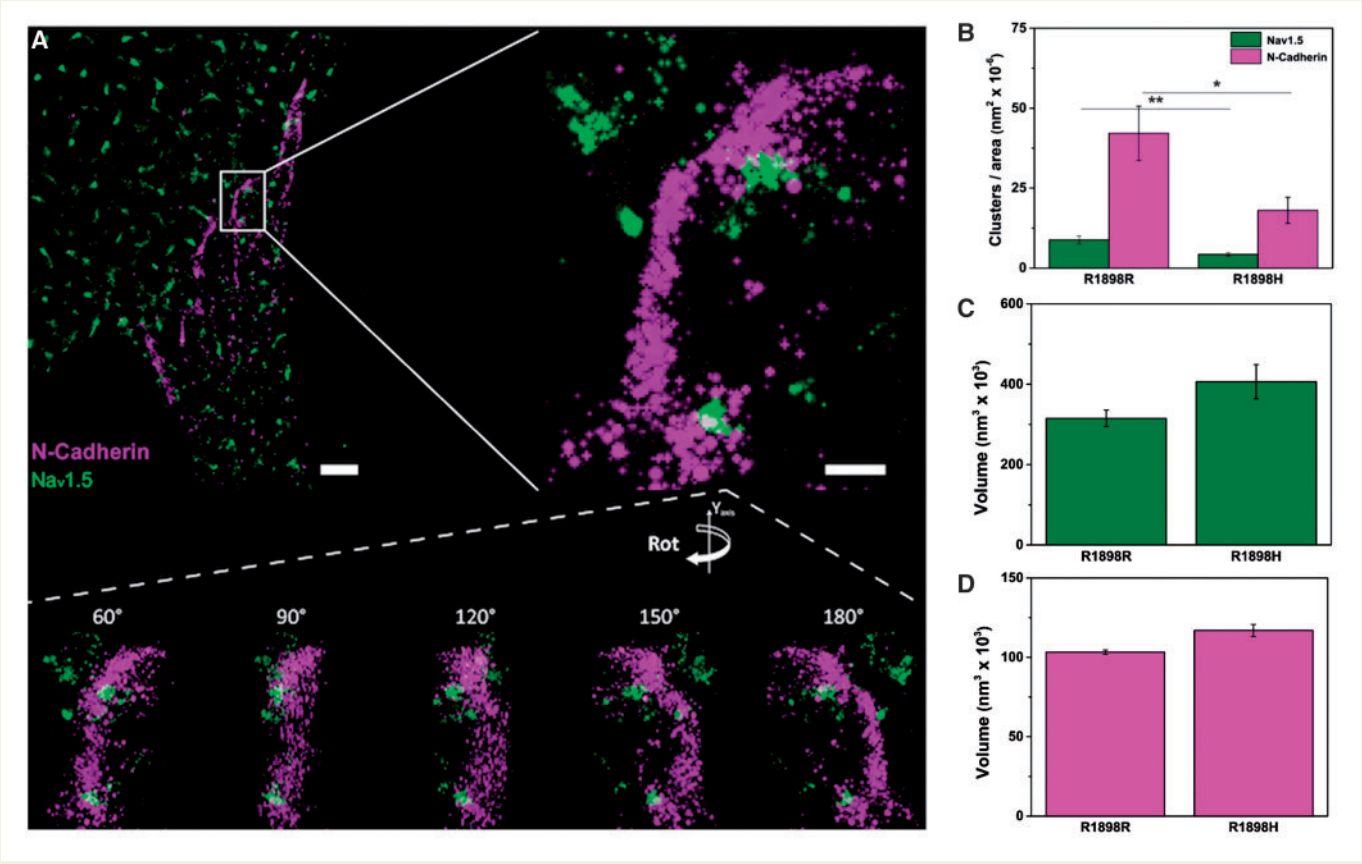

Figure 3 Effect of the *SCN5A* mutation on intercalated disc organization using super-resolution fluorescence microscopy. (*A*) 3D-SRFM image of IPSC-CMs stained for $Na_V1.5$ (green) and N-Cadherin (magenta). Top left panel shows a region of cell–cell contact. Inset images at the bottom show the interaction of the proteins at different *Y*-axis angle rotation. (*B–D*) 3D-SRFM cluster analysis of IPSC-CMs from ARVD/C patient cells (p.Arg1898His, R1898H) and gene-edited cells (p.Arg1898Arg, R1898R). (*B*) Cluster density of both $Na_v1.5$ (Green) and N-Cadherin (Magenta) was significantly higher in gene-edited cells [$4.27 \times 10^{-6} \pm 5.05 \times 10^{-7}$ (p.Arg1898His) vs. $8.80 \times 10^{-6} \pm 1.25 \times 10^{-6}$ (p.Arg1898Arg) for $Na_v1.5$, $P = 0.0054$; $18.03 \times 10^{-6} \pm 4.07 \times 10^{-6}$ (p.Arg1898His) vs. $42.16 \times 10^{-6} \pm 8.47 \times 10^{-6}$ (p.Arg1898Arg) for N-Cadherin, $P = 0.026$]. (*C*) Average $Na_v1.5$ cluster size was similar in both cell lines [406,386 ± 42,637 nm^3 (p.Arg1898His) vs. 315,359 ± 20,321 nm^3 (p.Arg1898Arg), $P = 0.126$]. (*D*) Average N-Cadherin cluster size was similar in both cell lines [116,893 ± 3901 nm^3 (p.Arg1898His) vs. 103,217 ± 1365 nm^3 (p.Arg1898Arg) $P = 0.536$]. p.Arg1898Arg, $n = 12$ images; 44480 $Na_v1.5$ clusters and 8268 N-Cadherin clusters. p.Arg1898His, $n = 10$ images; 9566 $Na_v1.5$ clusters and 44480 N-Cadherin clusters. All data are reported and analysed at the level of clusters. $^*P < 0.05$, $^{**}P = 0.005$ (statistics performed using Student's *t*-test).

Table S4, QRS duration was significantly prolonged in *SCN5A* variant carriers compared with all other ARVD/C subjects (119 ± 15 ms in *SCN5A* variant carriers vs. 94 ± 14 ms in others, $P < 0.01$). There were no significant differences in PR or QTc duration, or in any domain of the Task Force Criteria between the groups.

4. Discussion

This study represents the largest cohort of ARVD/C patients to date investigated for *SCN5A* mutations. Using hIPSC-CMs from an ARVD/C patient, we first defined the functional (patch clamp) and structural (3D-SRFM) effects caused by a single *SCN5A* mutation. Using gene editing, we were able to demonstrate that an amino acid substitution in $Na_v1.5$ not only has the (somewhat expected) repercussion of changing sodium current amplitude but also causes a structural deficit in the organization of a protein directly relevant to cell-adhesion (N-Cadherin). We subsequently screened 281 ARVD/C patients for *SCN5A* mutations, and showed that rare variants in *SCN5A* are present in approximately 2% of ARVD/C patients. Overall, these results support the notion that $Na_v1.5$ is in a functional complex with cell adhesion molecules, and reveal potential non-canonical mechanisms by which $Na_v1.5$ dysfunction may contribute to cardiomyopathy.

4.1 *SCN5A* mutations and $Na_v1.5$ function

4.1.1 Canonical $Na_v1.5$ function

Functional analyses were performed in an IPSC-CM cell model containing the *SCN5A* mutation (p.Arg1898His) observed in our discovery cohort. Super-resolution images show a normal cluster size, but reduced cluster density for $Na_v1.5$ at the intercalated disc, indicating that $Na_v1.5$ clusters are less abundant at the membrane. This suggests that the total I_{Na} that can potentially be generated is less, which is indeed confirmed by our whole-cell patch clamping results. Of note, the change in current amplitude was robust, and independent of cell type, as it was reproduced in an exogenous expression system.

Table 2 Clinical phenotype of five *SCN5A* variant carriers in the validation cohort

	p.Tyr416Cys	p.Leu729del	p.Arg1623Ter	p.Ser1787Asn	p.Val2016Met
Age at presentation (years)	52	24	23	32	37
Sex	Female	Male	Male	Male	Male
Ancestry	German/Italian	Dutch	Northern European	Ashkenazi Jewish	Dutch
Presentation	Palpitations	Sudden cardiac arrest	Sudden cardiac arrest	Palpitations	Ventricular tachycardia
Genetics					
Desmosomal mutation	–[a]	–	*PKP2* IVS10-1G>C	–	*PKP2* Trp676Ter
Task force criteria fulfilment					
Repolarization	V1–4 in presence CRBBB	TWI V1–3	TWI V1–3	TWI V1–3	TWI V1–2
Depolarization	None	Prolonged TAD	Prolonged TAD	Late potentials on SAECG	Prolonged TAD
Arrhythmia	LBI VT, 217 PVCs/24 h	LBS VT	LBI VT, 2297 PVCs/24 h	LBS VT, 1179 PVCs/24 h	LBS VT
Structural	Major	Major	Major	Major	Major
Family history	No	Yes	No	No	No
Conduction intervals					
PR (ms)	180	186	140	174	158
QRS (ms)	138	126	118	96	116
QTc (ms)	448	367	410	447	406
Clinical course					
Sustained VT/VF	No	Yes	Yes	Yes	Yes
Heart failure	No	No	Yes	No	No
Death	No	No	No	No	No

CRBBB, complete right bundle branch block; ECG, electrocardiogram; LBI, left bundle inferior; LBS, left bundle superior; VF, ventricular fibrillation; VT, ventricular tachycardia; *PKP2*, Plakophilin-2; PVC, premature ventricular complex; SAECG, signal-averaged ECG; TAD, terminal activation duration; TWI, T-wave inversion.
[a]The *SCN5A* p.Tyr416Cys carrier also carried a variant in *LMNA* [p.Arg190Gln (c.569G > A)]. Although SIFT and Polyphen2 classify this *LMNA* variant as damaging (score 0 and 1, respectively), and ClinVar reports on this variant as pathogenic, the literature on this variant is conflicting. Several sources classify the variant as likely polymorphism, given an UMD-predictor score 59 (probable polymorphism; http://www.umd.be/LMNA/4DACTION/WV/1705, accessed 22 July 2015), MutationAssessor score 2.76 (medium impact; http://mutationassessor.org/, accessed 22 July 2015), PANTHER score 0.675 (http://pantherdb.org/, accessed 22 July 2015), and SNP&GO classification as neutral (http://snps.biofold.org/snps-and-go/pages/method.html, accessed 22 July 2015). In addition, codon 190 seems to be a hotspot for variation, as other reports have described R190Q with reduced penetrance or with other mutations (Cenni *et al.*, *J Med Genet* 2005;42:214–20; Maraldi *et al.*, *Eur J Histochem* 2006;50:1–8); and co-segregation data were absent in two probands with R190Q as well as another LMNA mutation [Garcia-Pavia, *Eur Heart J* (abstract) http://eurheartj.oxfordjournals.org/content/ehj/34/suppl_1/P4234.full.pdf].

The p.Arg1898His mutation in our ARVD/C patient localizes to the $Na_v1.5$ C-terminal domain (CTD), a highly conserved region of the sodium channel that regulates channel function through many auxiliary proteins including Fibroblast Growth Factor 13 (FGF13; also known as fibroblast growth factor homologous factor 2) and calmodulin (CaM).[13] As shown in *Figure 5*, the mutated residue in our patient, p.Arg1898, sits at the hinge between the Na_v CTD and the IQ domain helix, where it interacts with the side chain of p.Glu1901 in the Na_v CTD and forms a cation-π interaction with the side chain of p.Tyr98 in FGF13. p.Tyr98 in FGF13 also interacts with p.Lys95 in CaM. Interestingly, sequence alignments indicate that p.Arg1898 in $Na_v1.5$ is homologous to p.Arg1902 in $Na_v1.2$, which, when mutated to Cys, has been associated with familial autism.[14] In $Na_v1.2$, the p.Arg1902Cys mutation leads to reduced binding of Ca^{2+}/CaM and thereby to abnormal Ca^{2+}-dependent regulation.[14,15] It is reasonable to think that a mutation of the equivalent residue in $Na_v1.5$, p.Arg1898, affects the same set of interactions, and therefore plays a similar role in the development of cardiac disease.

4.1.2 Non-canonical $Na_v1.5$ function

Although it is not surprising that a $Na_v1.5$ mutation causes sodium channel dysfunction, it is well recognized that *SCN5A* mutations may also lead to cardiac structural abnormalities.[16,17] However, the mechanism by which *SCN5A* mutations cause cardiomyopathy remains unknown. We recently described the presence of an adhesion/excitability node in cardiac myocytes.[8] In this prior work, we showed that (i) the adherens junction protein N-Cadherin serves as an attractor for $Na_v1.5$ clusters, (ii) the $Na_v1.5$ in these clusters are major determinants of the cardiac sodium current, and (iii) clustering of $Na_v1.5$ facilitates its regulation by molecular partners. In this study, we confirm and expand prior data by showing that $Na_v1.5$ is in a functional complex with cell adhesion molecules, and that a primary $Na_v1.5$ defect may affect N-Cadherin biology resulting in reduced size and density of N-Cadherin clusters at the intercalated disc. These results are particularly interesting in the context of prior studies showing that $Na_v1.5$ is delivered to the membrane via the microtubule network,[18] and that microtubules at the intercalated disc anchor at N-Cadherin-rich sites.[6,19] Whether $Na_v1.5$ interacts directly with N-Cadherin, or whether this interaction is mediated through unknown molecular partners remains currently unknown. Further investigation is warranted to establish the role of molecules at the $Na_v1.5$ CTD in orchestrating the interaction between mechanical and electrical junctions.

4.2 Prevalence and clinical implications of *SCN5A* mutations in ARVD/C

A previous study described *SCN5A* variants in 1 of 12 Chinese ARVD/C patients.[20] However, clinical data in this study were sparse and analyses were not corroborated by functional data. Our study shows that approximately 2% of ARVD/C cases harbour putatively pathogenic

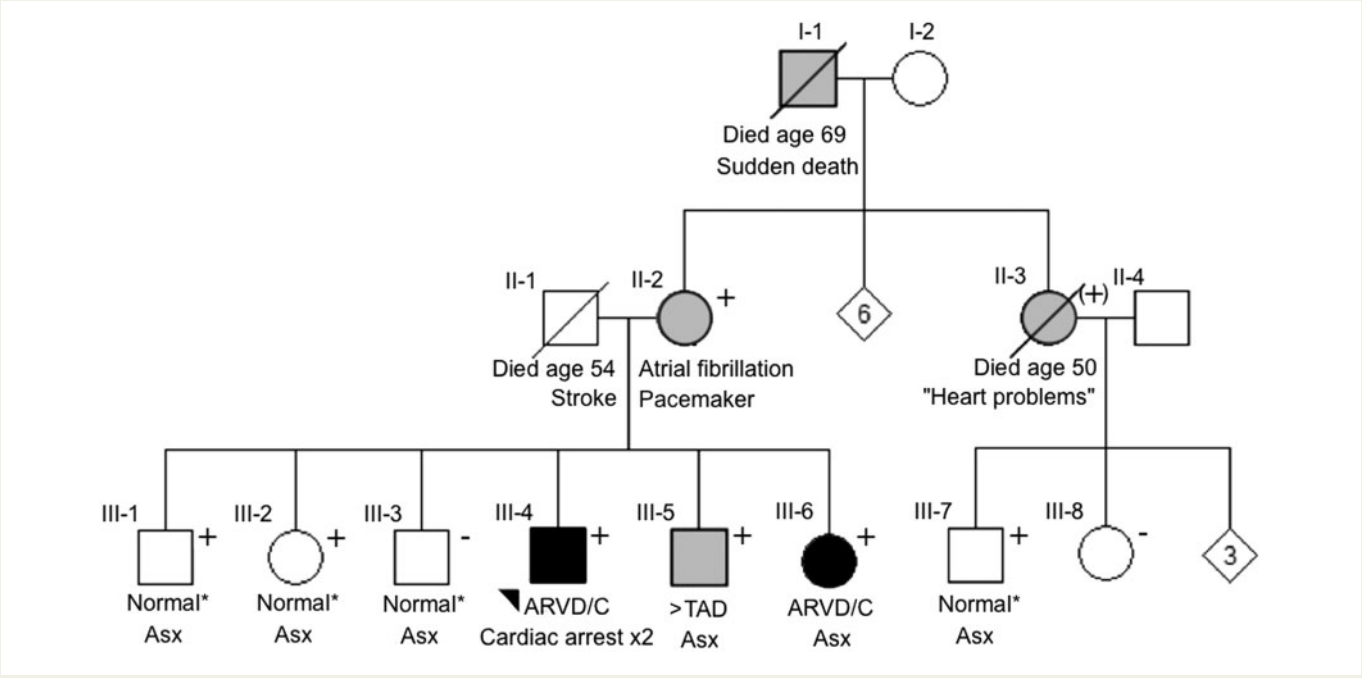

Figure 4 Pedigree of the p.Leu729del mutation carrier reveals co-segregation of the variant with the ARVD/C phenotype with reduced penetrance. The proband (III-4) is indicated with an arrowhead. The proband's mother (II-2) had atrial fibrillation and harboured the p.Leu729del variant. Among five siblings of the proband, four harboured the *SCN5A* variant, one of whom (III-6) was diagnosed with ARVD/C at age 34. Two siblings (III-1 and III-2) with the *SCN5A* variant were clinically unaffected at age 46 and 45. The 44-year-old male sibling without the *SCN5A* variant had a normal cardiac evaluation (III-3). The proband's grandfather (I-1) had sudden death at 69 years of age, but DNA was not available for testing. An aunt of the proband (II-3) was reported to have heart problems and was an obligate carrier of the mutation. Symbols: square: male, circle: female, +: *SCN5A* mutation carrier, (+): obligate *SCN5A* mutation carrier, solid: clinical ARVD/C diagnosis, grey: clinical symptoms and/or borderline ARVD/C diagnosis, empty: negative phenotype for ARVD/C. *No abnormalities on comprehensive cardiac evaluation including 12-lead electrocardiogram, Holter monitoring, and cardiac imaging. ARVD/C, arrhythmogenic right ventricular dysplasia/cardiomyopathy; ASx, asymptomatic; >TAD, prolonged terminal activation duration.

mutations in *SCN5A*. This yield is similar to the historical yield of 1–3% of other rare genes associated with ARVD/C.[1] One patient had an additional variant of uncertain significance in *LMNA* (*Table 2*). A pedigree can be found in the Supplementary material online, *Figure S2*. Her 33-year-old son had presyncope and palpitations, with frequent ventricular extrasystoles and borderline RV dimensions (RV end-diastolic volume 97.0 mL/m^2). He also harboured the *SCN5A*, but not the *LMNA*, variant. Although we cannot exclude the possibility that the *LMNA* variant contributes to this proband's phenotype, this highlights the well-established finding of multiple mutations in a subset of ARVD/C patients.[1,21]

As per study design, all individuals fulfilled diagnostic TFC for ARVD/C. In addition, each proband with an *SCN5A* mutation fulfilled major structural TFC for ARVD/C, further supporting the evidence that $Na_v1.5$ plays a role in cardiac structural integrity. Interestingly, QRS duration was significantly prolonged in *SCN5A* variant carriers compared with all other subjects, suggestive of a loss-of-function effect of $Na_v1.5$. Future studies are necessary to determine whether specific management recommendations should be made for ARVD/C patients with *SCN5A* variants. As in sodium channelopathies, avoidance of sodium channel blocking agents may prove to be prudent.

4.3 Implications for understanding of *SCN5A* pathophysiology

SCN5A mutations have been associated with a variety of clinical phenotypes including Brugada Syndrome,[22] Long QT Syndrome,[23] progressive cardiac conduction disease,[23] dilated cardiomyopathy,[16] and now also ARVD/C. Based on our results, we speculate that $Na_v1.5$ not only forms ion-selective pores but also is a multifunctional protein in a functional adhesion/excitability complex with mechanical junctions. Depending on the protein interaction affected, genetic changes in $Na_v1.5$ may thereby cause a predominantly structural phenotype (e.g. dilated cardiomyopathy), predominantly electrical phenotype (e.g. Brugada Syndrome, Long QT syndrome), or mixed electrical and structural phenotype (e.g. ARVD/C). As such, the affected protein interaction, more than the exact gene mutation, may determine the phenotype. Although further investigation is warranted to establish the role of auxiliary proteins in orchestrating the interaction between mechanical and electrical junctions at the intercalated disc, these data provide an additional explanation for the pathophysiological mechanism by which *SCN5A* mutations may result in cardiomyopathy.

4.4 Limitations

Recent studies have indicated that *SCN5A* has a 2–5% background rate of rare non-synonymous variants,[24] which complicates the interpretation of our results. Although the functional analyses (p.Arg1898His) and co-segregation data (p.Leu729del) in two of our patients support a deleterious, disease-causing effect, we were not able to obtain functional or segregation data for the other patients, However, all these mutations are radical or have previously been associated with disease.[22,25–29] Although all individuals in our study underwent genetic testing for the desmosomal

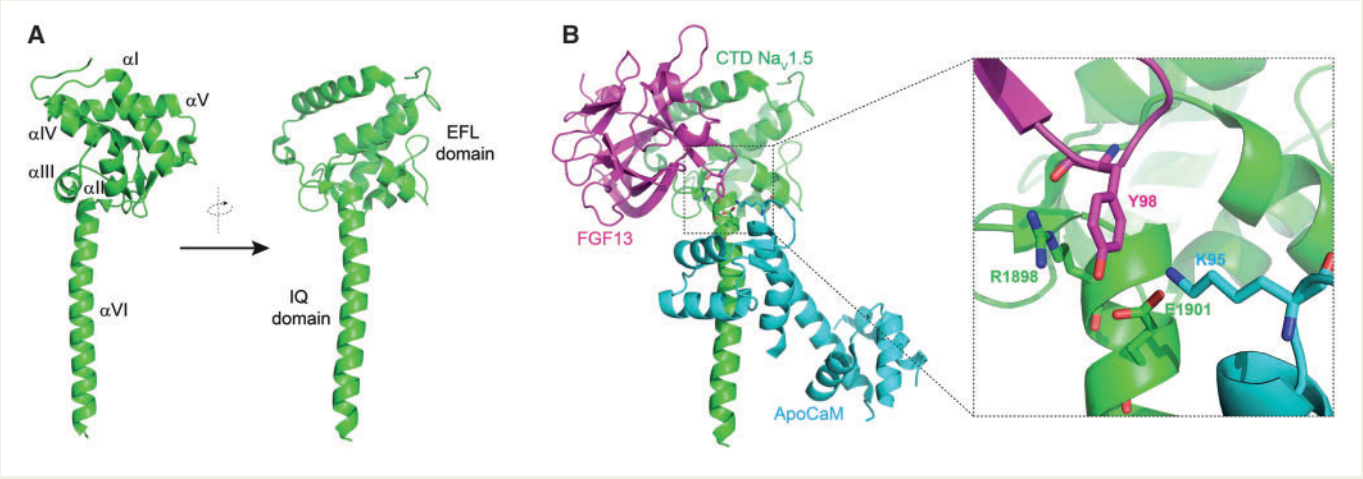

Figure 5 Crystal Structure of the $Na_v1.5$ C-Terminal Domain (CTD) (Green), FGF13 (Magenta), and ApoCaM (Cyan) complex. (*A*) Crystal structure of the $Na_v1.5$ CTD in cartoon representation. Annotations for all its six helices as well as for its domains containing the IQ and EFL motifs are shown. (*B*) Important residues for the interaction between the three molecules ($Na_v1.5$ CTD, FGF13, and ApoCaM) are shown in stick representation. The mutated residue in our patient (p.Arg1898 in $Na_v1.5$) is the only site in the ternary complex that unites all three molecules. p.Arg1898 interacts with the side chain of p.Glu1901 one turn below along the IQ domain helix of $Na_v1.5$ and also forms a cation-π interaction with the side chain of p.Tyr98 in FGF13. p.Glu1901 in the $Na_v1.5$ CTD and p.Tyr98 in FGF13 also interact with p.Lys95 within the third CaM EF-hand in the ApoCaM C-lobe through hydrogen bonds. ApoCaM, apocalmodulin; FGF13, fibroblast growth factor 13; PDB accession code 4DCK (Wang *et al.* 2014).[15]

genes, one-third [$n = 93/281$ (33%)] did not undergo whole-exome or large-panel-targeted sequencing, and mutations in genes infrequently associated with ARVD/C cannot be excluded in these individuals. Given the differences in screening methods, the finding of *SCN5A* variants in our validation cohort should be regarded as 'proof of principle' rather than definite evidence of pathogenicity in a single-gene Mendelian fashion.

IPSC-CMs are not fully mature cardiomyocytes: although these cells develop a contractile apparatus, the sarcomeres are disorganized and oriented in multiple directions. Also, IPSC-CMs do not have a proper mature intercalated disc structure connecting adjacent cells. As such, we focused our analysis on protein clusters in the immediate vicinity of the intercellular junction. In addition, it is important to note that statistical analyses on our IPSC-CMs and HEK293 cells are based on only one mutation. Although our study provides a possible explanation for the pathophysiological mechanism underlying structural changes in patients with an *SCN5A* mutation, it is important to recognize that many cardiac diseases associated with *SCN5A* do not exhibit structural abnormalities.

5. Conclusions

The results of our study show that putatively pathogenic *SCN5A* variants occur in approximately 2% of ARVD/C patients. *SCN5A* variants are associated with a significantly prolonged QRS duration. In one of our study subjects, we confirm a loss of $Na_v1.5$ function in two experimental systems. More importantly, we reveal reduced abundance of $Na_v1.5$ as well as N-Cadherin clusters at the intercalated disc, suggesting that $Na_v1.5$ is in a functional adhesion/excitability complex with mechanical junctions. Furthermore, our studies demonstrate the utility of the CRISPR/Cas9 technology in the phenotypical characterization of hIPSC-CMs containing suspect pathogenic substitutions. Overall, our data provide a novel, alternative explanation as to the pathophysiological mechanisms by which *SCN5A* mutations may cause a cardiomyopathic phenotype.

Supplementary material

Supplementary material is available at *Cardiovascular Research* online.

Acknowledgement

We are grateful to the ARVD/C patients and families who have made this work possible.

Funding

This work was supported by the Dutch Heart Foundation (2015T058 to A.S.J.M.t.R.); the Interuniversity Cardiology Institute of the Netherlands (project 06901); the Netherlands Cardiovascular Research Initiative of the Dutch Heart Foundation, Dutch Federation of University Medical Centres, the Netherlands Organization for Health Research and Development and the Royal Netherlands Academy of Sciences (CVON 2012-10 PREDICT to M.P.v.d.B., A.A.M.W., C.R.B., and J.P.V.T.); the American Heart Association (SDG 14SDG15850014 to M.C. and 15POST25550087 to E.A.-P.); Postdoctoral Fellowship to E.A.-P.; the National Institutes of Health (U54HG006542 and UL1TR001079, R01HL116906 to L.M., UL1RR025780 to L.M., R01HL69071 to L.M., K23JL067915 to M.R.G.T., R01HL109209 to M.R.G.T., HL106632-04 to M.D., and GM57691-17 to M.D.); the CRTrieste and Generali Assicurazioni Foundations (to G.S.); and the Children's Cardiomyopathy Foundation (to M.D.). The Johns Hopkins ARVD/C Program is supported by the Bogle Foundation, the Healing Hearts Foundation, the Campanella family, the Patrick J. Harrison Family, Dr Francis P. Chiaramonte Private Foundation, the Peter French Memorial Foundation, the Wilmerding Endowments, the Dr Satish, Rupal, and Robin Shah ARVD Fund at Johns Hopkins, the St Jude Medical Foundation, and Medtronic Inc.

Conflict of interest: none declared.

References

1. Groeneweg JA, Bhonsale A, James CA, Te Riele AS, Dooijes D, Tichnell C, Murray B, Wiesfeld AC, Sawant AC, Kassamali B, Atsma DE, Volders PG, de Groot NM, de Boer K, Zimmerman SL, Kamel IR, van der Heijden JF, Russell SD, Cramer MJ, Tedford RJ, Doevendans PA, van Veen TA, Tandri H, Wilde AA, Judge DP, van Tintelen JP, Hauer RN, Calkins H. Clinical presentation, long-term follow-up, and outcomes of 1001 arrhythmogenic right ventricular dysplasia/cardiomyopathy patients and family members. *Circ Cardiovasc Genet* 2015;**8**:437–446.
2. Kaplan SR, Gard JJ, Protonotarios N, Tsatsopoulou A, Spiliopoulou C, Anastasakis A, Squarcioni CP, McKenna WJ, Thiene G, Basso C, Brousse N, Fontaine G, Saffitz JE. Remodeling of myocyte gap junctions in arrhythmogenic right ventricular cardiomyopathy due to a deletion in plakoglobin (naxos disease). *Heart Rhythm* 2004;**1**:3–11.
3. Cerrone M, Noorman M, Lin X, Chkourko H, Liang FX, van der Nagel R, Hund T, Birchmeier W, Mohler P, van Veen TA, van Rijen HV, Delmar M. Sodium current deficit and arrhythmogenesis in a murine model of plakophilin-2 haploinsufficiency. *Cardiovasc Res* 2012;**95**:460–468.
4. Noorman M, Hakim S, Asimaki A, Vreeker A, van Rijen HV, van der Heyden MA, de Jonge N, de Weger RA, Hauer RN, Saffitz JE, van Veen TA. Reduced plakoglobin immunoreactivity in arrhythmogenic cardiomyopathy: methodological considerations. *Cardiovasc Pathol* 2013;**22**:314–318.
5. Sato PY, Coombs W, Lin X, Nekrasova O, Green KJ, Isom LL, Taffet SM, Delmar M. Interactions between ankyrin-g, plakophilin-2, and connexin43 at the cardiac intercalated disc. *Circ Res* 2011;**109**:193–201.
6. Cerrone M, Lin X, Zhang M, Agullo-Pascual E, Pfenniger A, Chkourko Gusky H, Novelli V, Kim C, Tirasawadichai T, Judge DP, Rothenberg E, Chen HS, Napolitano C, Priori SG, Delmar M. Missense mutations in plakophilin-2 cause sodium current deficit and associate with a brugada syndrome phenotype. *Circulation* 2014;**129**:1092–1103.
7. Noorman M, Hakim S, Kessler E, Groeneweg JA, Cox MG, Asimaki A, van Rijen HV, van Stuijvenberg L, Chkourko H, van der Heyden MA, Vos MA, de Jonge N, van der Smagt JJ, Dooijes D, Vink A, de Weger RA, Varro A, de Bakker JM, Saffitz JE, Hund TJ, Mohler PJ, Delmar M, Hauer RN, van Veen TA. Remodeling of the cardiac sodium channel, connexin43, and plakoglobin at the intercalated disk in patients with arrhythmogenic cardiomyopathy. *Heart Rhythm* 2013;**10**:412–419.
8. Leo-Macias A, Agullo-Pascual E, Sanchez-Alonso JL, Keegan S, Lin X, Arcos T, Feng Xia L, Korchev YE, Gorelik J, Fenyo D, Rothenberg E, Rothenberg E, Delmar M. Nanoscale visualization of functional adhesion/excitability nodes at the intercalated disc. *Nat Commun* 2016;**7**:10342.
9. Marcus FI, McKenna WJ, Sherrill D, Basso C, Bauce B, Bluemke DA, Calkins H, Corrado D, Cox MG, Daubert JP, Fontaine G, Gear K, Hauer R, Nava A, Picard MH, Protonotarios N, Saffitz JE, Sanborn DM, Steinberg JS, Tandri H, Thiene G, Towbin JA, Tsatsopoulou A, Wichter T, Zareba W. Diagnosis of arrhythmogenic right ventricular cardiomyopathy/dysplasia: proposed modification of the task force criteria. *Eur Heart J* 2010;**31**:806–814.
10. UCSC Genome Browser. Accessible via https://genome.ucsc.edu (30 July 2016, date last accessed).
11. Bhonsale A, Groeneweg JA, James CA, Dooijes D, Tichnell C, Jongbloed JD, Murray B, Te Riele AS, van den Berg MP, Bikker H, Atsma DE, de Groot NM, Houweling AC, van der Heijden JF, Russell SD, Doevendans PA, van Veen TA, Tandri H, Wilde AA, Judge DP, van Tintelen JP, Calkins H, Hauer RN. Impact of genotype on clinical course in arrhythmogenic right ventricular dysplasia/cardiomyopathy-associated mutation carriers. *Eur Heart J* 2015;**36**:847–855.
12. Ran FA, Hsu PD, Wright J, Agarwala V, Scott DA, Zhang F. Genome engineering using the crispr-cas9 system. *Nat Protoc* 2013;**8**:2281–2308.
13. Wang C, Hennessey JA, Kirkton RD, Wang C, Graham V, Puranam RS, Rosenberg PB, Bursac N, Pitt GS. Fibroblast growth factor homologous factor 13 regulates Na+ channels and conduction velocity in murine hearts. *Circ Res* 2011;**109**:775–782.
14. Weiss LA, Escayg A, Kearney JA, Trudeau M, MacDonald BT, Mori M, Reichert J, Buxbaum JD, Meisler MH. Sodium channels scn1a, scn2a and scn3a in familial autism. *Mol Psychiatry* 2003;**8**:186–194.
15. Wang C, Chung BC, Yan H, Wang HG, Lee SY, Pitt GS. Structural analyses of Ca(2)(+)/cam interaction with Nav channel c-termini reveal mechanisms of calcium-dependent regulation. *Nat Commun* 2014;**5**:4896.
16. Olson TM, Keating MT. Mapping a cardiomyopathy locus to chromosome 3p22-p25. *J Clin Invest* 1996;**97**:528–532.
17. Olson TM, Michels VV, Ballew JD, Reyna SP, Karst ML, Herron KJ, Horton SC, Rodeheffer RJ, Anderson JL. Sodium channel mutations and susceptibility to heart failure and atrial fibrillation. *JAMA* 2005;**293**:447–454.
18. Casini S, Tan HL, Demirayak I, Remme CA, Amin AS, Scicluna BP, Chatyan H, Ruijter JM, Bezzina CR, van Ginneken AC, Veldkamp MW. Tubulin polymerization modifies cardiac sodium channel expression and gating. *Cardiovasc Res* 2010;**85**:691–700.
19. Shaw RM, Fay AJ, Puthenveedu MA, von Zastrow M, Jan YN, Jan LY. Microtubule plus-end-tracking proteins target gap junctions directly from the cell interior to adherens junctions. *Cell* 2007;**128**:547–560.
20. Yu J, Hu J, Dai X, Cao Q, Xiong Q, Liu X, Liu X, Shen Y, Chen Q, Hua W, Hong K. Scn5a mutation in Chinese patients with arrhythmogenic right ventricular dysplasia. *Herz* 2014;**39**:271–275.
21. Rigato I, Bauce B, Rampazzo A, Zorzi A, Pilichou K, Mazzotti E, Migliore F, Marra MP, Lorenzon A, De Bortoli M, Calore M, Nava A, Daliento L, Gregori D, Iliceto S, Thiene G, Basso C, Corrado D. Compound and digenic heterozygosity predicts lifetime arrhythmic outcome and sudden cardiac death in desmosomal gene-related arrhythmogenic right ventricular cardiomyopathy. *Circ Cardiovasc Genet* 2013;**6**:533–542.
22. Kapplinger JD, Tester DJ, Alders M, Benito B, Berthet M, Brugada J, Brugada P, Fressart V, Guerchicoff A, Harris-Kerr C, Kamakura S, Kyndt F, Koopmann TT, Miyamoto Y, Pfeiffer R, Pollevick GD, Probst V, Zumhagen S, Vatta M, Towbin JA, Shimizu W, Schulze-Bahr E, Antzelevitch C, Salisbury BA, Guicheney P, Wilde AA, Brugada R, Schott JJ, Ackerman MJ. An international compendium of mutations in the scn5a-encoded cardiac sodium channel in patients referred for brugada syndrome genetic testing. *Heart Rhythm* 2010;**7**:33–46.
23. Postema PG, Van den Berg M, Van Tintelen JP, Van den Heuvel F, Grundeken M, Hofman N, Van der Roest WP, Nannenberg EA, Krapels IP, Bezzina CR, Wilde A. Founder mutations in the Netherlands: Scn5a 1795insd, the first described arrhythmia overlap syndrome and one of the largest and best characterised families worldwide. *Neth Heart J* 2009;**17**:422–428.
24. Le Scouarnec S, Karakachoff M, Gourraud JB, Lindenbaum P, Bonnaud S, Portero V, Duboscq-Bidot L, Daumy X, Simonet F, Teusan R, Baron E, Violleau J, Persyn E, Bellanger L, Barc J, Chatel S, Martins R, Mabo P, Sacher F, Haissaguerre M, Kyndt F, Schmitt S, Bezieau S, Le Marec H, Dina C, Schott JJ, Probst V, Redon R. Testing the burden of rare variation in arrhythmia-susceptibility genes provides new insights into molecular diagnosis for brugada syndrome. *Hum Mol Genet* 2015;**24**:2757–2763.
25. Ackerman MJ, Splawski I, Makielski JC, Tester DJ, Will ML, Timothy KW, Keating MT, Jones G, Chadha M, Burrow CR, Stephens JC, Xu C, Judson R, Curran ME. Spectrum and prevalence of cardiac sodium channel variants among Black, White, Asian, and Hispanic individuals: implications for arrhythmogenic susceptibility and brugada/long qt syndrome genetic testing. *Heart Rhythm* 2004;**1**:600–607.
26. Hu RM, Tan BH, Tester DJ, Song C, He Y, Dovat S, Peterson BZ, Ackerman MJ, Makielski JC. Arrhythmogenic biophysical phenotype for scn5a mutation s1787n depends upon splice variant background and intracellular acidosis. *PLoS One* 2015;**10**:e0124921.
27. Splawski I, Shen J, Timothy KW, Lehmann MH, Priori S, Robinson JL, Moss AJ, Schwartz PJ, Towbin JA, Vincent GM, Keating MT. Spectrum of mutations in long-qt syndrome genes. Kvlqt1, herg, scn5a, kcne1, and kcne2. *Circulation* 2000;**102**:1178–1185.
28. Chen J, Makiyama T, Wuriyanghai Y, Ohno S, Sasaki K, Hayano M, Harita T, Nishiuchi S, Yuta Y, Ueyama T, Shimizu A, Horie M, Kimura T. Cardiac sodium channel mutation associated with epinephrine-induced qt prolongation and sinus node dysfunction. *Heart Rhythm* 2016;**13**:289–298.
29. Shy D, Gillet L, Ogrodnik J, Albesa M, Verkerk AO, Wolswinkel R, Rougier JS, Barc J, Essers MC, Syam N, Marsman RF, van Mil AM, Rotman S, Redon R, Bezzina CR, Remme CA, Abriel H. Pdz domain-binding motif regulates cardiomyocyte compartment-specific nav1.5 channel expression and function. *Circulation* 2014;**130**:147–160.
30. Saguner AM, Ganahl S, Kraus A, Baldinger SH, Medeiros-Domingo A, Saguner AR, Mueller-Burri SA, Wolber T, Haegeli LM, Krasniqi N, Tanner FC, Steffel J, Brunckhorst C, Duru F. Clinical role of atrial arrhythmias in patients with arrhythmogenic right ventricular dysplasia. *Circ J* 2014;**78**:2854–2861.
31. Nagase S, Kusano KF, Morita H, Nishii N, Banba K, Watanabe A, Hiramatsu S, Nakamura K, Sakuragi S, Ohe T. Longer repolarization in the epicardium at the right ventricular outflow tract causes type 1 electrocardiogram in patients with brugada syndrome. *J Am Coll Cardiol* 2008;**51**:1154–1161.